



1 A Fortran-Python Interface for Integrating Machine Learning Parameterization into  
2 Earth System Models

3  
4 Tao Zhang<sup>1</sup>, Cyril Morcrette<sup>2,7</sup>, Meng Zhang<sup>3</sup>, Wuyin Lin<sup>1</sup>, Shaocheng Xie<sup>3</sup>, Ye Liu<sup>4</sup>, Kwinten Van  
5 Weverberg<sup>5,6</sup>, Joana Rodrigues<sup>2</sup>

- 6  
7 1. Brookhaven National Laboratory, Upton, NY, USA  
8 2. Met Office, FitzRoy Road, Exeter, EX13PB, UK  
9 3. Lawrence Livermore National Laboratory, Livermore, CA, USA  
10 4. Pacific Northwest National Laboratory, Richland, WA, USA  
11 5. Department of Geography, Ghent University, Belgium  
12 6. Royal Meteorological Institute of Belgium, Brussels, Belgium  
13 7. Department of Mathematics and Statistics, Exeter University, Exeter, UK

14  
15 Correspondence to: Tao Zhang (taozhang.ccs@gmail.com)

16 **Abstract**

17  
18 Parameterizations in Earth System Models (ESMs) are subject to biases and uncertainties arising from  
19 subjective empirical assumptions and incomplete understanding of the underlying physical processes.  
20 Recently, the growing representational capability of machine learning (ML) in solving complex problems  
21 has spawned immense interests in climate science applications. Specifically, ML-based parameterizations  
22 have been developed to represent convection, radiation and microphysics processes in ESMs by learning  
23 from observations or high-resolution simulations, which have the potential to improve the accuracies and  
24 alleviate the uncertainties. Previous works have developed some surrogate models for these processes  
25 using ML. These surrogate models need to be coupled with the dynamical core of ESMs to investigate  
26 the effectiveness and their performance in a coupled system. In this study, we present a novel Fortran-  
27 Python interface designed to seamlessly integrate ML parameterizations into ESMs. This interface  
28 showcases high versatility by supporting popular ML frameworks like PyTorch, TensorFlow, and Scikit-  
29 learn. We demonstrate the interface's modularity and reusability through two cases: a ML trigger function  
30 for convection parameterization and a ML wildfire model. We conduct a comprehensive evaluation of  
31 memory usage and computational overhead resulting from the integration of Python codes into the



32 Fortran ESMs. By leveraging this flexible interface, ML parameterizations can be effectively developed,  
33 tested, and integrated into ESMs.  
34

## 35 Plain Language

36 Earth System Models (ESMs) are crucial for understanding and predicting climate change. However, they  
37 struggle to accurately simulate the climate due to uncertainties associated with parameterizing sub-grid  
38 physics. Although higher-resolution models can reduce some uncertainties, they require significant  
39 computational resources. Machine learning (ML) algorithms offer a solution by learning the important  
40 relationships and features from high-resolution models. These ML algorithms can then be used to develop  
41 parameterizations for coarser-resolution models, reducing computational and memory costs. To  
42 incorporate ML parameterizations into ESMs, we develop a Fortran-Python interface that allows for  
43 calling Python functions within Fortran-based ESMs. Through two case studies, this interface  
44 demonstrates its feasibility, modularity and effectiveness.

## 45 1. Introduction

46 Earth System Models (ESMs) play a crucial role in understanding the mechanism of the climate system  
47 and projecting future changes. However, uncertainties arising from parameterizations of sub-grid  
48 processes pose challenges to the reliability of model simulations (Hourdin et al., 2017). Kilometer-scale  
49 high-resolution models (Schär et al., 2020) can potentially mitigate the uncertainties by directly resolving  
50 some key subgrid-scale processes that need to be parameterized in conventional low-resolution ESMs.  
51 Another promising method, superparameterization – a type of multi-model framework (MMF) (D.  
52 Randall et al., 2003; D. A. Randall, 2013), explicitly resolves sub-grid processes by embedding high-  
53 resolution cloud-resolved models within the grid of low-resolution models. Consequently, both high-  
54 resolution models and superparameterization approaches have shown promise in improving the  
55 representation of cloud formation and precipitation. However, their implementation is challenged by  
56 exceedingly high computational costs.

57

58 In recent years, machine learning (ML) techniques have emerged as a promising approach to  
59 improve parameterizations in ESMs. They are capable of learning complex patterns and  
60 relationships directly from observational data or high-resolution simulations, enabling the  
61 capture of nonlinearities and intricate interactions that may be challenging to represent with



62 traditional parameterizations. For example, Zhang et al. (2021) proposed a ML trigger function  
63 for a deep convection parameterization by learning from field observations, demonstrating its  
64 superior accuracy compared to traditional CAPE-based trigger functions. Chen et al. (2023)  
65 developed a neural network-based cloud fraction parameterization, better predicting both spatial  
66 distribution and vertical structure of cloud fraction when compared to the traditional Xu-Randall  
67 scheme (Xu & Randall, 1996). Krasnopolsky et al. (2013) prototyped a system using a neural  
68 network to learn the convective temperature and moisture tendencies from cloud-resolving  
69 model (CRM) simulations. These tendencies refer to the rates of change of various atmospheric  
70 variables over one time step, diagnosed from particular parameterization schemes. These studies  
71 lay the groundwork for integrating ML-based parameterization into ESMs.

72

73 However, the aforementioned studies primarily focus on offline ML of parameterizations that do  
74 not directly interact with ESMs. Recently, there have been efforts to implement ML  
75 parameterizations that can be directly coupled with ESMs. Several studies have developed ML  
76 parameterizations in ESMs by hard coding custom neural network modules, such as O’Gorman  
77 & Dwyer (2018), Rasp et al. (2018), Han et al. (2020) and Gettelman et al. (2021). They  
78 incorporated a Fortran-based ML inference module to allow the loading of the pre-trained ML  
79 weights to reconstruct the ML algorithm in ESMs. The hard-coding has limitations. Kochkov et  
80 al. (2023) presented an innovative ML parameterization that feeds back from the dynamics, in  
81 order to improve stability and reduce bias. However, such hard-coding approach restricts the ML  
82 algorithm’s ability to adapt to changes in the model dynamics over time, as the ‘online’ updating  
83 requires a two-way coupling between the dominantly Fortran-based ESMs and Python ML  
84 libraries.

85

86 Fortran-Keras Bridge (FKB; Ott et al. (2020)) and C Foreign Function Interface (CFFI;  
87 <https://cffi.readthedocs.io>) are two packages that support two-way coupling between Fortran-based ESM  
88 and Python based ML parameterizations. FKB enables tight integration of Keras deep learning models but  
89 is specifically bound to the Keras library, limiting its compatibility with other frameworks like PyTorch  
90 and Scikit-Learn. On the other hand, CFFI provides a more flexible solution that in principle supports  
91 coupling various ML packages due to its language-agnostic design. Brenowitz & Bretherton (2018)  
92 utilized it to enable the calling of Python ML algorithms within ESMs. However, the CFFI has several  
93 limitations. When utilizing CFFI to interface Fortran and Python, it uses global data structures to pass



94 variables between the two languages. This approach results in additional memory overhead as variable  
95 values need to be copied between languages, instead of being passed by reference. Additionally, CFFI  
96 lacks automatic garbage collection for the unused memory within these data structures and copies.  
97 Consequently, the memory usage of the program gradually increases over its lifetime. In addition, when  
98 using CFFI to call Python functions from a Fortran program, the process involves several steps such as  
99 registering variables into a global data structure, calling the Python function, and retrieving the calculated  
100 result. These multiple steps can introduce computational overhead due to the additional operations  
101 required.

102

103 Additionally, Wang et al. (2022) developed a coupler to facilitate two-way communication between ML  
104 parameterizations and host ESMs. The coupler gathers state variables from the ESM using the Message  
105 Passing Interface (MPI) and transfers them to a Python-based ML module. It then receives the output  
106 from the Python code and returns them to the ESM. While this approach effectively bridges Fortran and  
107 Python, its use of file-based data passing to exchange information between modules carries some  
108 performance overhead relative to tighter coupling techniques. Optimizing the data transfer, such as via  
109 shared memory, remains an area for improvement to fully leverage this coupler's ability to integrate  
110 online-adaptive ML parameterizations within large-scale ESM simulations, which is the main goal for this  
111 study.

112

113 In this study, we investigate the integration of ML parameterizations into Fortran-based ESM  
114 models by establishing a flexible interface that enables the invocation of ML algorithms in  
115 Python from Fortran. This integration offers access to a diverse range of ML frameworks,  
116 including PyTorch, TensorFlow, and Scikit-learn, which can effectively be utilized for  
117 parameterizing intricate atmospheric and other climate system processes. The coupling of the  
118 Fortran model and the Python ML code needs to be performed for thousands of model columns  
119 and over thousands of timesteps for a typical model simulation. Therefore, it is crucial for the  
120 coupling interface to be both robust and efficient. We showcase the feasibility and benefits of  
121 this approach through case studies that involve the parameterization of deep convection and  
122 wildfire processes in ESMs. The two cases demonstrate the robustness and efficiency of the  
123 coupling interface. The focus of this paper is on documenting the coupling between the Fortran  
124 ESM and the ML algorithms and systematically evaluating the computational efficiency and  
125 memory usage of different ML frameworks (such as Pytorch and TensorFlow), different ML  
126 algorithms, and different configuration of a climate model. The assessment of the scientific



127 performance of the ML emulators will be addressed in follow-on papers. The showcase examples  
128 emphasize the potential for high modularity and reusability by separating the ML components  
129 into Python modules. This modular design facilitates independent development and testing of  
130 ML-based parameterizations by researchers. It enables easier code maintenance, updates, and the  
131 adoption of state-of-the-art ML techniques without disrupting the existing Fortran infrastructure.  
132 Ultimately, this advancement will contribute to enhanced predictions and a deeper  
133 comprehension of the evolving climate of our planet.

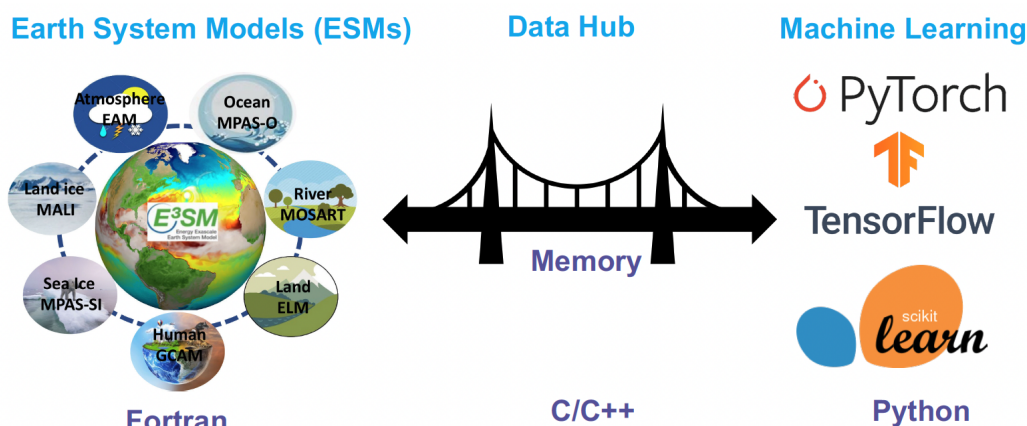
134

135 The rest of this manuscript is organized as follows: Section 2 presents the detailed interface that  
136 integrates ML into Fortran-based ESM models. Section 3 discusses the performance of the  
137 interface and presents its application in two case studies. Finally, Section 4 provides a summary  
138 of the findings and a discussion of their implications.

## 139 2. General design of the ML interface

### 140 2.1 Architecture of the ML interface

141 We developed an interface using shared memory to enable two-way coupling between Fortran and Python  
142 (Figure 1). The ESM used in the demonstration in Figure 1 is the U.S. Department of Energy (DOE)  
143 Energy Exascale Earth System Model (E3SM; Golaz et al., 2019, 2022). Because Fortran cannot directly  
144 call Python, we utilized C as an intermediary since Fortran can call C functions. This approach leverages  
145 C as a data hub to exchange information without requiring a framework-specific binding like KFB. As a  
146 result, our interface supports invoking any Python-based ML package such as PyTorch, TensorFlow, and  
147 scikit-learn from Fortran. While C can access Python scalar values through the built-in  
148 PyObject\_CallObject function from the Python C API, we employed Cython for its ability to transfer  
149 array data between the languages. Using Cython, multidimensional data structures can be efficiently  
150 passed between Fortran and Python modules via C, allowing for flexible training of ML algorithms within  
151 ESMs.



152

153 **Figure 1.** The interface of the ML bridge for two-way communication via memory between Fortran ESM  
154 and Python ML module. The diagram for the ESMs uses E3SM as an illustration. Note that MALI and  
155 GCAM are yet active components of officially released E3SM.

## 156 2.2 Code structure

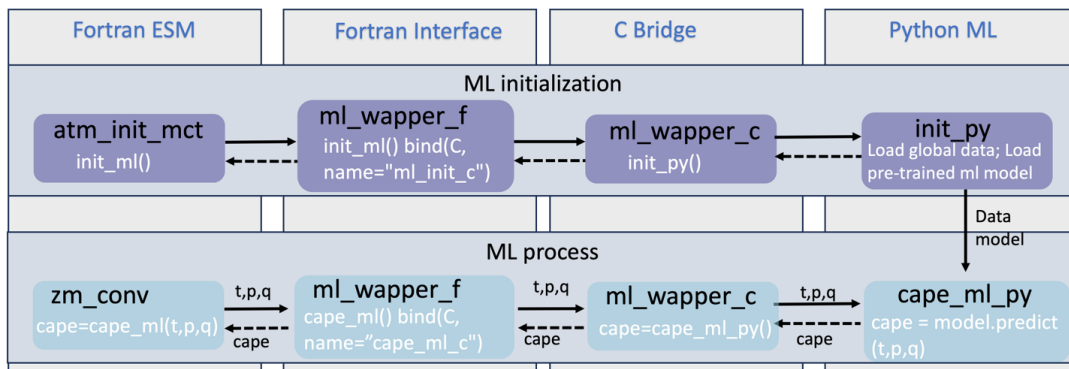
157 Figure 2 illustrates the structure of the ML bridge interface as applied to E3SM. The interface consists of  
158 four main components: the Fortran ESM, Fortran Interface, C Bridge, and Python ML. The ML functions  
159 are invoked within the original Fortran ESM parameterization components, such as the atmospheric  
160 convection and microphysics modules. This process involves transferring the required input variables to  
161 Python and defining the expected output variables to be returned to the Fortran component. The Fortran  
162 Interface and C Bridge play a crucial role in establishing the interface between Fortran and Python. They  
163 facilitate the transfer of variables between Fortran and Python by utilizing memory references. The ML  
164 function called within the Fortran ESM is defined in the Fortran interface, which is then bound to a  
165 corresponding C function. This seamless integration enables efficient communication and data exchange  
166 between the Fortran and Python components. The Python ML component is responsible for handling ML-  
167 related tasks, such as loading the trained ML algorithm and using it to make predictions. Cython is used  
168 to simplify the usage and facilitate the transfer and return of arrays. It allows for efficient integration of  
169 Python code with C libraries, enhancing performance and enabling seamless array operations within the  
170 ML component.

171

172 The interface consists of two stages. The first stage involves initializing the ML environment, which  
173 persists throughout the model simulations. On the Fortran ESM side, the `init_ml()` function is called in the  
174 `atm_init_mct` module. Through the Fortran Interface and C Bridge, the corresponding function in the



175 Python ML component is invoked. This function loads the ML-related global data and the trained ML  
 176 algorithm. This initialization process is performed only once to enhance efficiency and avoid unnecessary  
 177 repetition during the simulations. The second stage involves the actual invocation of the ML process. The  
 178 example here is an ML-based closure for the deep convection parameterization. We aim to utilize ML to  
 179 calculate Convective Available Potential Energy (CAPE) by utilizing an ML emulator based on high-  
 180 resolution cloud-resolving model simulations. We call the `cape_ml` function in the Fortran module  
 181 `zm_conv`, providing temperature, pressure, and humidity as input variables, and defining the returned  
 182 CAPE from the ML side. Through the Fortran Interface and C Bridge, these three variables are passed to  
 183 the Python ML component. In the Python ML component, the received variables, along with other pre-  
 184 loaded global data and the trained ML algorithm, are used to calculate the ML-based CAPE. The  
 185 calculated result is then returned to the Fortran ESM. The Fortran ESM utilizes this ML-derived CAPE to  
 186 determine how convection will evolve.  
 187  
 188

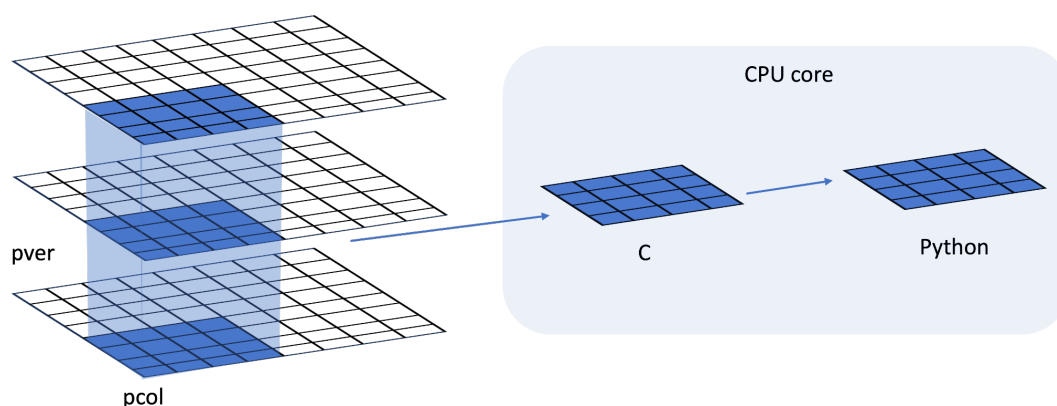


189  
 190 **Figure 2.** The code structure of the ML bridge interface using the ML closure in deep convection as an  
 191 example.

192  
 193 In traditional ESMs, sub-grid scale parameterization routines such as convection parameterizations are  
 194 often calculated separately for each vertical column of the model domain. Meanwhile, the domain is  
 195 typically decomposed horizontally into 2D chunks that can be solved in parallel using MPI processes.  
 196 Each CPU core/MPI process is assigned a number of chunks of model columns to update asynchronously  
 197 (Figure 3). Our interface takes advantage of this existing parallel decomposition by designing the ML  
 198 calls to operate over all columns simultaneously within each chunk, rather than invoking the ML scheme  
 199 individually for each column. This allows the coupled model-ML system to leverage parallelism in the  
 200 neural network computations. If the ML were called separately for every column, parallel efficiencies



201 would not be realized. By aggregating inputs over the chunk-scale prior to interfacing with Python,  
202 performance is improved through better utilization of multi-core and GPU-based ML capabilities during  
203 parameterization calculations. The Python, C, Cython and Fortran code components are compiled  
204 together into a unified executable file. Table 1 shows the detailed steps to enable the ML bridge interface  
205 in E3SM.  
206



207  
208 **Figure 3.** Data and system structure. The model domain is decomposed into chunks of columns. pver  
209 refers to number of pressure vertical levels. A chunk contains multiple columns (up to pcol). Multiple  
210 chunks can be assigned to each CPU core.  
211  
212

**Table 1.** The steps to enable the ML bridge framework in E3SM

Step	Description
1.	Create the Python environment using Conda <ul style="list-style-type: none"><li>• conda create ML4ESM</li><li>• conda activate ML4ESM</li></ul>
2.	Add the Python ML environment in the compile CMake file
3.	Incorporate the ML bridge framework codes (including the Fortran Interface and C Bridge) into the ESM codebase.





4. Initialize of ML environment by loading necessary global data and the pre-trained ML algorithm.
5. Implement the ML prediction and the transmission of the resulting values to the ESM parameterization module.
6. Cythonize the Python code
7. Build and compile the ESM
8. Submit the job for model simulation

213

### 214 3. Results

215 The framework explained in the previous section provides seamless support for various ML  
216 parameterizations and various ML frameworks, such as PyTorch, Tensorflow, and Scikit-learn. To  
217 demonstrate the versatility of this framework, we applied it two distinct case applications. The first  
218 application replaces the conventional CAPE-based trigger function in deep convection parameterization  
219 with a machine-learned trigger function. The second application involves a ML-based wildfire model that  
220 interacts bidirectionally with the ESM. We provide a brief introduction to these two cases. Detailed  
221 descriptions and evaluations will be presented in separate papers.

222

223 The framework's performance is influenced by two primary factors: increasing memory usage and  
224 increasing computational overhead. Firstly, maintaining the Python environment fully persistent in  
225 memory throughout model simulations can impact memory usage, especially for large ML algorithms.  
226 This elevated memory footprint increases the risk of leaks or crashes as simulations progress. Secondly,  
227 executing ML components within the Python interpreter inevitably introduces some overhead compared  
228 to the original ESMs. The increased memory requirements and decreased computational efficiency  
229 associated with these considerations can impact the framework's usability, flexibility, and scalability for  
230 different applications.

231



232 To comprehensively assess performance, we conducted a systematic evaluation of various ML  
233 frameworks, ML algorithms, and physical models. This evaluation is built upon the foundations  
234 established for evaluating the ML trigger function in the deep convection parameterization.

### 235 3.1 Application cases

#### 236 3.1.1 ML trigger function in deep convection parameterization

237 Convection plays a vital role in atmospheric processes, such as precipitation formation, heat and moisture  
238 transport, and energy redistribution (Arakawa, 2004; Arakawa & Schubert, 1974). However, the  
239 deficiencies in convection parameterizations constitute one of the principal sources of uncertainties in  
240 General Circulation Models (D. A. Randall, 2013). Some uncertainties in convection parameterizations  
241 are recognized to be closely linked to the convection trigger function used in these schemes (Bechtold et  
242 al., 2004; Xie et al., 2004, 2019; Xie & Zhang, 2000; Lee et al., 2007). The convective trigger in a  
243 convective parameterization determines when and where model convection should be triggered as the  
244 simulation advances. In many convection parameterizations, the trigger function consists of a simple,  
245 arbitrary threshold for a physical quantity, such as convective available potential energy (CAPE).  
246 Figure 4a illustrates how the CAPE-based trigger function works. Convection will be triggered if the  
247 CAPE value exceeds a threshold value, such as 70 J/kg used in E3SM version 1.

248

249 In this work, we develop a ML trigger function and apply it to E3SM (Golaz et al., 2019, 2022). A brief  
250 overview of this ML trigger function is given here, while further details will be elaborated upon in a  
251 subsequent paper. The training data originates from simulations performed using the Met Office Unified  
252 Model Regional Atmosphere 1.0 configuration (Bush et al., 2020). Each simulation consists of a limited  
253 area model (LAM) nested within a global forecast model providing boundary conditions (Walters et al.,  
254 2017; Webster et al., 2008). In total 80 LAM simulations were run located so as to sample different  
255 geographical regions worldwide. Each LAM was run for 1 month, with 2-hourly output, using a grid-  
256 length of 1.5 km, a 512 x 512 domain, and a model physics package used for operational weather  
257 forecasting. This physics package does not include a convective parameterization scheme, but does  
258 include a representation of fractional cloudiness (Bush et al., 2020). The 1.5 km data is coarse-grained to  
259 several scales from 15 to 144 km, comparable to the scale a global model might be run at. At each scale,  
260 we assess whether individual pixels can be considered to be buoyant cloudy updrafts (BCU, e.g.  
261 Hartmann et al., 2019; Swann, 2001). Here, the threshold for buoyant is local virtual temperature more  
262 than 0.1 K warmer than the average at that scale and height. Cloudy is defined whenever the fractional  
263 cloud cover is greater than 0.0 and updraft is defined as vertical ascent larger than 0.2 m/s. In each



264 averaging region, the number of grid points that meet all three criteria are counted and saved as a profile  
265 of BCU fraction.

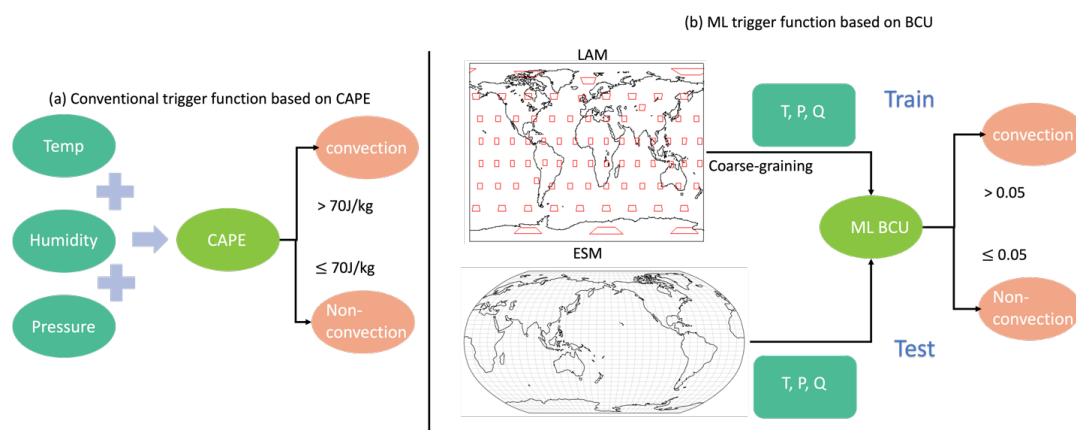
266

267 A two-stream neural network architecture is used for the ML model. The first stream takes profiles of  
268 temperature, specific humidity and pressure as inputs and passes them through a 4-layer convolutional  
269 neural network (CNN) with kernel sizes of 3, to extract large scale features. The second stream takes  
270 mean orographic height, standard deviation of orographic height, land fraction and the size of the grid-  
271 box as inputs. The outputs of the two streams are then combined and fed into a 2-layer fully connected  
272 network to allow the ML model to leverage both atmospheric and surface features when making its  
273 predictions. The output of the ML model is a profile of BCU.

274

275 Once trained, the CNN is coupled to E3SM and thermodynamic information from E3SM is passed to it to  
276 predict the profile of BCU. If there are 3 contiguous levels where the predicted BCU is larger than 0.05,  
277 the convection scheme is triggered.

278



279

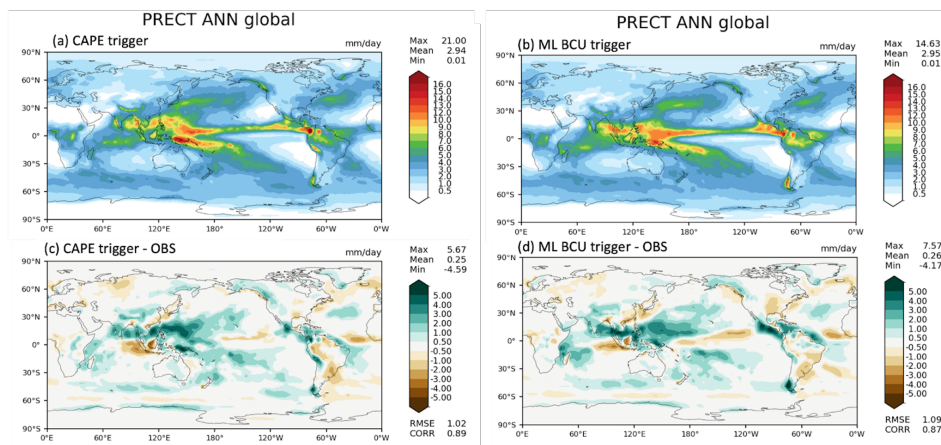
280 **Figure 4.** Structure of traditional CAPE-based and the new ML BCU-based trigger function. The  
281 rectangles in LAM represent the LAM domains.

282

283 The ML trigger function is implemented using this two-stream architecture and coupled with the E3SM  
284 model using the framework described in Section 2. Figure 5 shows the comparison of annual mean  
285 precipitation between the control run using the CAPE-based trigger function and the run using the ML  
286 BCU trigger function. The ML BCU scheme demonstrates reasonable spatial patterns of precipitation,  
287 similar to the control run, with comparable root-mean-square error and spatial correlation. Additional



288 experiments exploring the definition of BCU and varying the thresholds along with an in-depth analysis  
289 will be presented in a follow-up paper.  
290



291  
292 **Figure 5.** Comparison of annual mean precipitation between the control run using the CAPE-based  
293 trigger function (a, c) and the run using the ML BCU trigger function (b, d).  
294

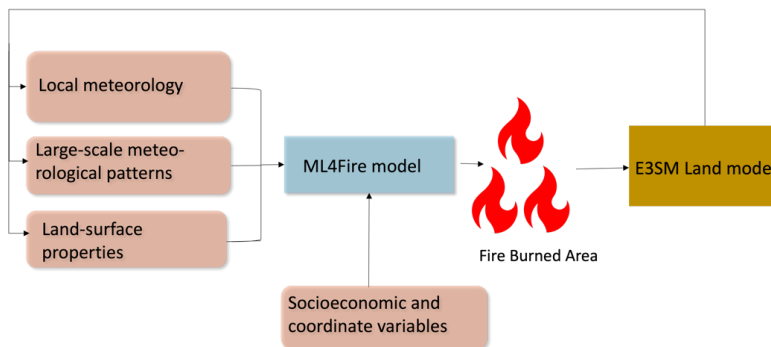
### 295 3.1.2 ML learning fire model

296 Wildfires in the United States have significantly increased in frequency and intensity in recent decades,  
297 resulting in substantial direct and indirect losses (Iglesias et al., 2022). Predicting wildfire burned area is  
298 challenging due to the complex interrelationships between fires, climate, weather, vegetation, topography,  
299 and human activities (Huang et al., 2020). Traditionally, statistical methods like multiple linear regression  
300 have been applied, but are limited in the number and diversity of predictors considered (Yue et al., 2013).  
301 Alternatively, ML algorithms that capture statistical relationships between the burned area and  
302 environmental factors have shown promising burned area prediction (Kondylatos et al., 2022; Li et al.,  
303 2023; Wang et al., 2022, 2023). However, improving long-term burned area projections and evaluating  
304 fire impacts requires the coupling of the fire model to an earth system model, which allows simulations of  
305 the interactions between the fire, atmosphere, land cover and vegetation (Huang et al., 2021). To achieve  
306 this, we develop a coupled fire-land-atmosphere framework using ML.

307  
308 The ML algorithm is trained using a monthly dataset, which includes the target variable of burned area, as  
309 well as various predictor variables. These predictors encompass local meteorological data (e.g., surface  
310 temperature, precipitation), land surface properties (e.g., monthly mean evapotranspiration and surface

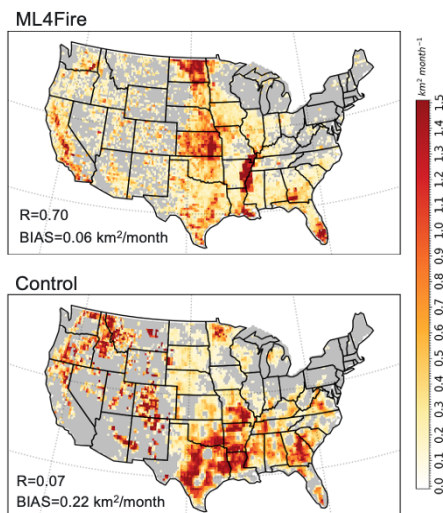


311 soil moisture), and socioeconomic variables (e.g., gross domestic product, population density), as  
312 described by Wang et al. (2022). In the coupled fire-land-atmosphere framework, meteorology variables  
313 and land surface properties are provided by the E3SM, as illustrated in Figure 6. We use the eXtreme  
314 Gradient Boosting algorithm implemented in Scikit-Learn to train the ML fire model. Figure 7  
315 demonstrates that the ML4Fire model exhibits superior performance in terms of spatial distribution  
316 compared to process-based fire models, particularly in the Southern US region. Detailed analysis will be  
317 presented in a separate paper. The ML4Fire model has proven to be a valuable tool for studying  
318 vegetation-fire interactions, enabling seamless exploration of climate-fire feedbacks.



319  
320  
321

**Figure 6.** Structure of ML fire model (ML4Fire) coupled into E3SM model.



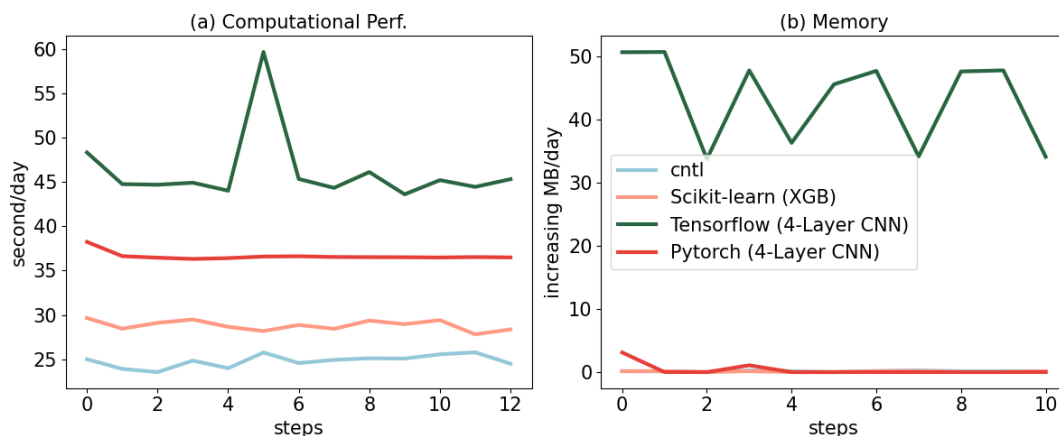
322

323 **Figure 7.** Comparison between ML4Fire model and process-based fire model against the historical  
324 burned area from Global Fire Emissions Database 5 from 2001-2020. R and BIAS are the spatial  
325 pattern correlation and difference against the observation, respectively.



### 326 3.2 Performance of different ML frameworks

327 The Fortran-Python bridge ML interface supports various ML frameworks, including PyTorch,  
328 TensorFlow, and scikit-learn. These ML frameworks can be trained offline using kilometer-scale high-  
329 resolution models (such as the ML trigger function) or observations (ML fire model). Once trained, they  
330 can be plugged into the ML bridge interface through different API interfaces specific to each framework.  
331 The coupled ML algorithms are persistently resident in memory, just like the other ESM components.  
332 During each step of the process, the performance of the full system is significantly affected by memory  
333 usage. If memory consumption increases substantially, it may lead to memory leaks as the number of time  
334 step iteration increases. In addition, Python, being an interpreted language, is typically considered to have  
335 slower performance compared to compiled languages like C/C++ and Fortran. Therefore, incorporating  
336 Python may decrease computational performance. We examine the memory usage and computational  
337 performance across various ML frameworks based on implementing the ML trigger function in E3SM.  
338 The ML algorithm is implemented as a two-stream CNN model using Pytorch and TensorFlow  
339 frameworks, as well as XGBoost using the Scikit-learn package.



340  
341 **Figure 8.** Computational and memory overhead as the simulation progresses for coupling the ML trigger  
342 function with the E3SM model. The x-axis represents the simulated time step. The y-axis of (a) represents  
343 the simulation speed measured in seconds per day (indicating the number of seconds required to simulate  
344 one day). The y-axis of (b) represents the relative increase in memory usage for Scikit-learn, TensorFlow,  
345 and PyTorch compared with CNTL. CNTL represents the original simulation without using the ML  
346 framework.

347  
348 Figure 8 illustrates the computational and memory overhead associated with the ML parameterization  
349 using different ML frameworks. It shows that XGBoost only exhibits a 20% increase in the simulation  
350 time required for simulating one day due to its simpler algorithm. For more complex neural networks,



351 PyTorch incurs a 52% overhead, while TensorFlow's overhead is almost 100% – about two times as much  
352 as the overhead by PyTorch. In terms of memory usage, we use the highwater memory metric (Gerber &  
353 Wasserman, 2013), which represents the total memory footprint of a process. Scikit-learn and PyTorch do  
354 not show any significant increase in memory usage. However, TensorFlow shows a considerable increase  
355 up to 50MB per simulation day per MPI process element. This is significant because for a node with 48  
356 cores, it would equate to an increase of around 2GB per simulated day on that node. This rapid memory  
357 growth could quickly lead to a simulation crash due to insufficient memory during continuous  
358 integrations, preventing the use in practical simulations. Our findings show that the TensorFlow  
359 prediction function does not release memory after each call. Therefore, we recommend using PyTorch for  
360 complex deep learning algorithms and Scikit-learn for simpler ML algorithms to avoid these potential  
361 memory-related issues when using TensorFlow.

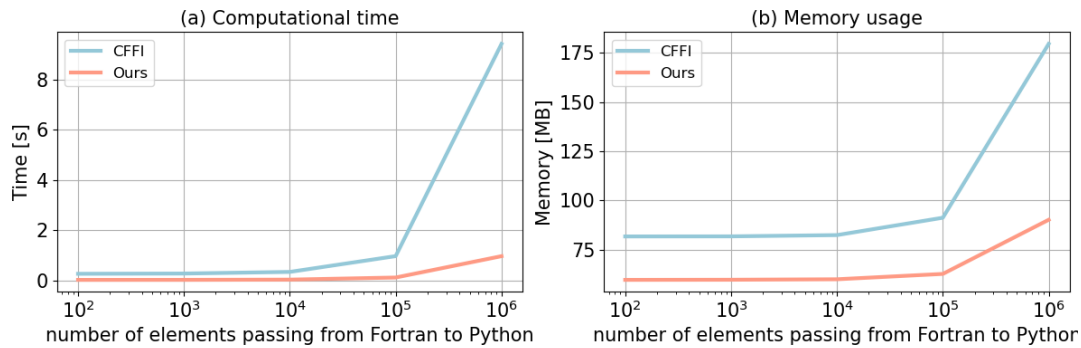
362

363 Previous work, such as Brenowitz & Bretherton (2018, 2019) has utilized the CFFI package to establish  
364 communication between Fortran ESM and ML Python. As described in the Introduction, while CFFI  
365 offers flexibility in supporting various ML packages, it does have certain limitations. To pass variables  
366 from Fortran to Python, the approach relies on global data structures to store all variables, including both  
367 the input from Fortran to Python and the output returning to Fortran. Consequently, this package results in  
368 additional memory copy operations and increasing overall memory usage. In contrast, our interface takes  
369 a different approach by utilizing memory references to transfer data between Fortran and Python,  
370 avoiding the need for global data structures and the associated overhead. This allows for a more efficient  
371 data transfer process.

372

373 In Figure 9, we present a comparison between the two frameworks by testing the different number of  
374 elements passed from Fortran to Python. The evaluation is based on a demo example that focuses solely  
375 on declaring arrays and transferring them from Fortran to Python, rather than a real E3SM simulation.  
376 Figure 9a illustrates the impact of the number of passing elements on the overhead of the two interfaces.  
377 As the number of elements exceeds  $10^4$ , the overhead of CFFI becomes significant. When the number  
378 surpasses  $10^6$ , the overhead of CFFI is nearly ten times greater than that of our interface. Regarding  
379 memory usage, our interface maintains a stable memory footprint of approximately 60MB. Even as the  
380 number of elements increases, the memory usage only shows minimal growth. However, for CFFI, the  
381 memory usage starts at 80MB, which is 33% higher than our interface. As the number of elements  
382 reaches  $10^6$ , the memory overhead for CFFI dramatically rises to 180MB, twice as much as our interface.

383



384  
 385 Figure 9. Comparison of our framework and the CFFI framework in terms of computational time  
 386 and memory usage. The x-axis represents the number of elements transferred from Fortran to  
 387 Python, while the y-axis displays the total time (a) and total memory usage (b) for a  
 388 demonstration example. The evaluations presented are based on the average results obtained  
 389 from 5 separate tests.  
 390

### 391 3.3 Performance of ML algorithms of different complexities

392 ML parameterizations can be implemented using various deep learning algorithms with different levels of  
 393 complexity. The computational performance and memory usage can be influenced by the complexity of  
 394 these algorithms. In the case of the ML trigger function, a two-stream four-layer CNN structure is  
 395 employed. We compare this structure with other ML algorithms such as Artificial Neural Network (ANN)  
 396 and Residual Network (ResNet), whose structures are detailed in Table 2. These algorithms are  
 397 implemented in PyTorch. The algorithm’s complexity is measured by the number of parameters, with the  
 398 CNN having approximately 60 times more parameters than ANN, and ResNet having roughly 1.5 times  
 399 more parameters than CNN.

400  
 401 **Table 2.** The structure and number of parameters of each ML algorithms.

Algorithms	Structure	# of parameters
ANN	3 x Linear	121,601
CNN	4 x Conv2d + 2 x Linear	7,466,753
ResNet	17 x Conv2d + 1 x Linear	11,177,025



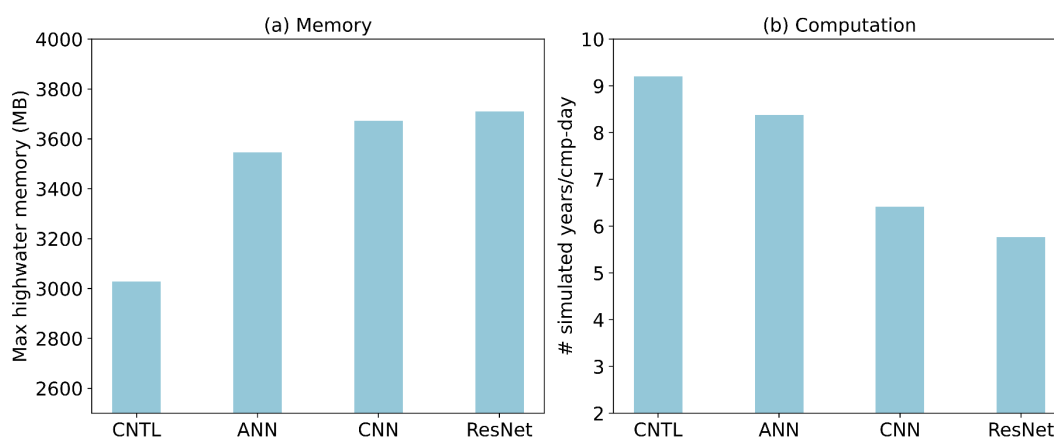


402

403 Figure 10 presents a comparison of the memory and computational costs between the CNTL run without  
404 deep learning parameterization and various deep learning algorithms. A same specific process-element  
405 layout (placement of ESM component models on distributed CPU cores) is used for all the simulations.  
406 Deep learning algorithms incur a significant yet affordable increase in memory overhead, with at least a  
407 20% increase compared to the CNTL run (Figure 10a). This is primarily due to the integration of ML  
408 algorithms into the ESM, which persist throughout the simulations. Although there is a notable increase in  
409 complexity among the deep learning algorithms, their memory usage only shows a slight rise. This is  
410 because the memory increment resulting from the ML parameters is relatively small. Specifically, ANN  
411 requires 1MB of memory, CNN requires 60MB, and the ResNet algorithms requires 85MB, which are  
412 calculated based on the number of parameters in each algorithm. When comparing these values to the  
413 memory consumption of the CNTL run, which is approximately 3000MB, the additional parameters'  
414 incremental memory consumption is not substantial.

415

416 However, there is a significant decrease in computational performance as the complexity of the deep  
417 learning algorithms increases (Figure 10b). This is primarily due to the larger number of parameters in  
418 neural networks, which require more forward computations. It is worth noting that in this study, the deep  
419 learning algorithms are executed on CPUs. To enhance computational performance, future work could  
420 consider utilizing GPUs for acceleration.



421

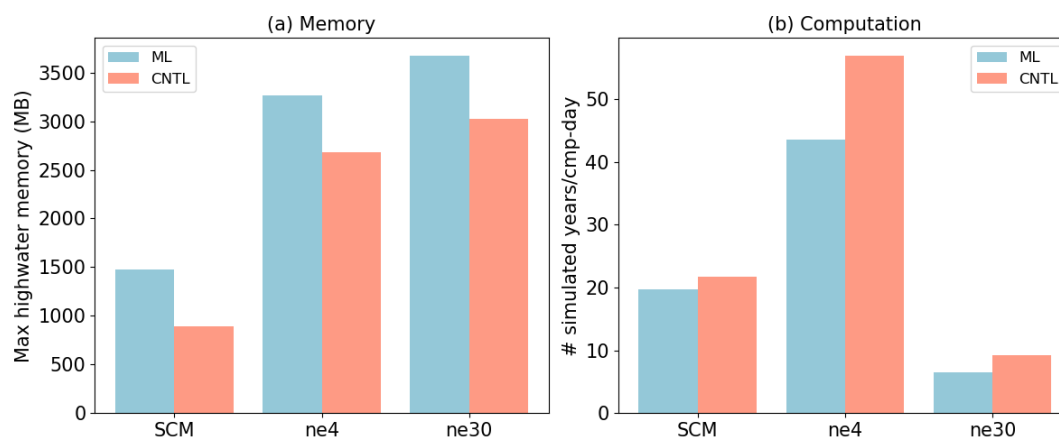
422 **Figure 10.** Comparison of CNTL and various ML algorithms in terms of memory and computation.

423 CNTL is the default run without ML parameterizations.

424



### 425 3.4 Performance for physical models of different complexities



426  
427 **Figure 11.** Comparison CNTL and ML for various ESMs in terms of memory and computation. The  
428 ESM configuration include SCM, ultra-low resolution model (ne4) and nominal low-resolution model  
429 (ne30).

430  
431 ML parameterization can be applied to various ESM configurations, for example, with the E3SM  
432 Atmosphere Model (EAM), we experiment with Single Column Model (SCM), the ultra low-resolution  
433 model of EAM (ne4), and the nominal low resolution model of EAM (ne30) configurations. The SCM  
434 consists of one single atmosphere column of a global EAM (Bogenschutz et al., 2020; Gettelman et al.,  
435 2019). ne4 has 384 columns, with each column representing the horizontal resolution of 7.5°. ne30 is the  
436 default resolution for EAM and comprises 21,600 columns, with each column representing the horizontal  
437 resolution of 1°. In the case of the ML trigger function, the memory overhead is approximately 500MB  
438 for all configurations due to the loading of the ML algorithm, which does not vary with the configuration  
439 of the ESM.

440  
441 Regarding computational performance, SCM utilizes 1 process, ne4 employs 1 node with 64 processes,  
442 and ne30 utilizes 10 nodes with each node using 128 processes. In the case of SCM, the overhead  
443 attributed to the ML parameterization is approximately 9% due to the utilization of only 1 process.  
444 However, for ne4 and ne30, the overhead is 23% and 28% respectively (Figure 11). The increasing  
445 computational overhead is primarily due to resource competition when multiple processes are used within  
446 a single node.

447



## 448 4. Discussion and Conclusion

449 In this study, we develop a novel Fortran-Python interface for developing ML parameterizations. ML  
450 algorithm can learn detailed information about cloud processes and atmospheric dynamics from  
451 kilometer-scale models and observations and serves as an approximate surrogate for the kilometer-scale  
452 model. Instead of explicitly simulating kilometer-scale processes, the ML algorithms can be designed to  
453 capture the essential features and relationships between atmospheric variables by training on available  
454 kilometer-scale data. The trained algorithms can then be used to develop parameterizations for use in  
455 models at coarser resolutions, reducing the computational and memory costs. By using ML  
456 parameterizations, scientists can effectively incorporate the insights gained from kilometer-scale models  
457 for coarser-resolution simulations. Through learning the complex relationships and patterns present in the  
458 high-resolution data, the ML-based parameterizations have the potentials to more accurately represent  
459 cloud processes and atmospheric dynamics in the ESMs. This approach strikes a balance between  
460 computational efficiency and capturing critical processes, enabling more realistic simulations and  
461 predictions while minimizing computational resources. All these potential benefits in turn promote  
462 innovative developments to facilitate increasing and more efficient use of ML parameterizations.

463  
464 In this study, we develop a novel Fortran-Python interface for developing ML parameterizations. This  
465 interface demonstrates feasibility in supporting various ML frameworks, such as PyTorch, TensorFlow,  
466 and Scikit-learn and enables the effective development of new ML-based parameterizations to explore  
467 ML-based applications in ESMs. Through two cases - a ML trigger function in convection  
468 parameterization and a ML wildfire model - we highlight high modularity and reusability of the  
469 framework. We conduct a systematic evaluation of memory usage and computational overhead from the  
470 integrated Python codes.

471  
472 Based on our performance evaluation, we observe that coupling ML algorithms using TensorFlow into  
473 ESMs can lead to memory leaks. As a recommendation, we suggest using PyTorch for complex deep  
474 learning algorithms and Scikit-learn for simple ML algorithms for the Fortran-Python ML interface.

475  
476 The memory overhead primarily arises from loading ML algorithms into ESMs. If the ML algorithms are  
477 implemented using PyTorch or Scikit-learn, the memory usage will not increase significantly. The  
478 computational overhead is influenced by the complexity of the neural network and the number of  
479 processes running on a single node. As the complexity of the neural network increases, more parameters



480 in the neural network require gradient computation. Similarly, when there are more processes running on  
481 a single node, the integrated Python codes introduces more resource competition.

482

483 Although this interface provides a flexible tool for ML parameterizations, it does not currently utilize  
484 GPUs for ML algorithms. In Figure 3, it is shown that each chunk is assigned to a CPU core. However, to  
485 effectively leverage GPUs, it is necessary to gather the variables from multiple chunks and pass them to  
486 the GPUs. Additionally, if an ESM calls the Python ML module multiple times in each time step, the  
487 computational overhead becomes significant. It is crucial to gather the variables and minimize the number  
488 of calls. In the future, we will enhance the framework to support this mechanism, enabling GPU  
489 utilization and overall performance improvement.

## 490 Acknowledge

491 This work was primarily supported by the Energy Exascale Earth System Model (E3SM) project of the  
492 Earth and Environmental System Modeling program, funded by the US Department of Energy, Office of  
493 Science, Office of Biological and Environmental Research. Research activity at BNL was under the  
494 Brookhaven National Laboratory contract DE-SC0012704 (Tao Zhang, Wuyin Lin). The work at LLNL  
495 was performed under the auspices of the US Department of Energy by the Lawrence Livermore National  
496 Laboratory under Contract DE-AC52-07NA27344. The work at PNNL is performed under the Laboratory  
497 Directed Research and Development Program at the Pacific Northwest National Laboratory. PNNL is  
498 operated by DOE by the Battelle Memorial Institute under contract DE-A05-76RL01830.

499

## 500 Author contribution

501 TZ developed the Fortran-Python Interface. CM and JR contributed the ML model for the trigger  
502 function. YL contributed the ML model for the wire fire model. TZ and MZ assessed the performance of  
503 the ML trigger function. TZ took the lead in preparing the manuscript, with valuable edits from CM, MZ,  
504 WL, SX, YL, KW, and JR. All the co-authors provided valuable insights and comments for the  
505 manuscript.

## 506 Conflict of Interest

507 The authors declare that they have no conflict of interest.

508



## 509 Data Availability Statement

510 The Fortran-Python interface for developing ML parameterizations can be archived at  
511 <https://doi.org/10.5281/zenodo.11005103> (Zhang et al., 2024). The E3SM model can be accessed at  
512 <https://doi.org/10.11578/E3SM/dc.20240301.3> (E3SM Project, 2024).

## 513 References

- 514 Bechtold, P., Chaboureaud, J.-P., Beljaars, A., Betts, A. K., Köhler, M., Miller, M., & Redelsperger, J.-L.  
515 (2004). The simulation of the diurnal cycle of convective precipitation over land in a global  
516 model. *Quarterly Journal of the Royal Meteorological Society*, *130*(604), 3119–3137.  
517 <https://doi.org/10.1256/qj.03.103>
- 518 Bogenschutz, P. A., Tang, S., Caldwell, P. M., Xie, S., Lin, W., & Chen, Y.-S. (2020). The E3SM version  
519 1 single-column model. *Geoscientific Model Development*, *13*(9), 4443–4458.  
520 <https://doi.org/10.5194/gmd-13-4443-2020>
- 521 Brenowitz, N. D., & Bretherton, C. S. (2018). Prognostic validation of a neural network unified physics  
522 parameterization. *Geophysical Research Letters*, *45*(12), 6289–6298.  
523 <https://doi.org/10.1029/2018gl078510>
- 524 Brenowitz, N. D., & Bretherton, C. S. (2019). Spatially extended tests of a neural network  
525 parametrization trained by coarse-graining. *Journal of Advances in Modeling Earth Systems*,  
526 *11*(8), 2728–2744. <https://doi.org/10.1029/2019ms001711>
- 527 Bush, M., Allen, T., Bain, C., Boutle, I., Edwards, J., Finnenkoetter, A., Franklin, C., Hanley, K., Lean,  
528 H., Lock, A., Manners, J., Mittermaier, M., Morcrette, C., North, R., Petch, J., Short, C., Vosper,  
529 S., Walters, D., Webster, S., ... Zerroukat, M. (2020). The first Met Office Unified Model–  
530 JULES Regional Atmosphere and Land configuration, RAL1. *Geoscientific Model Development*,  
531 *13*(4), 1999–2029. <https://doi.org/10.5194/gmd-13-1999-2020>
- 532 Chen, G., Wang, W., Yang, S., Wang, Y., Zhang, F., & Wu, K. (2023). A Neural Network-Based Scale-  
533 Adaptive Cloud-Fraction Scheme for GCMs. *Journal of Advances in Modeling Earth Systems*,  
534 *15*(6), e2022MS003415. <https://doi.org/10.1029/2022MS003415>



- 535 Covey, C., Gleckler, P. J., Doutriaux, C., Williams, D. N., Dai, A., Fasullo, J., Trenberth, K., & Berg, A.  
536 (2016). Metrics for the Diurnal Cycle of Precipitation: Toward Routine Benchmarks for Climate  
537 Models. *Journal of Climate*, 29(12), 4461–4471. <https://doi.org/10.1175/JCLI-D-15-0664.1>  
538 E3SM Project. (2024). *Energy Exascale Earth System Model v3.0.0* [Computer software].  
539 <https://doi.org/10.11578/E3SM/DC.20240301.3>
- 540 Gerber, R., & Wasserman, H. (2013). *High Performance Computing and Storage Requirements for*  
541 *Biological and Environmental Research Target 2017* (LBNL-6256E). Lawrence Berkeley  
542 National Lab. (LBNL), Berkeley, CA (United States). <https://doi.org/10.2172/1171504>
- 543 Gettelman, A., Gagne, D. J., Chen, C.-C., Christensen, M. W., Lebo, Z. J., Morrison, H., & Gantos, G.  
544 (2021). Machine Learning the Warm Rain Process. *Journal of Advances in Modeling Earth*  
545 *Systems*, 13(2), e2020MS002268. <https://doi.org/10.1029/2020MS002268>
- 546 Gettelman, A., Truesdale, J. E., Bacmeister, J. T., Caldwell, P. M., Neale, R. B., Bogenschutz, P. A., &  
547 Simpson, I. R. (2019). The Single Column Atmosphere Model Version 6 (SCAM6): Not a Scam  
548 but a Tool for Model Evaluation and Development. *Journal of Advances in Modeling Earth*  
549 *Systems*, 11(5), 1381–1401. <https://doi.org/10.1029/2018MS001578>
- 550 Golaz, J.-C., Caldwell, P. M., Van Roekel, L. P., Petersen, M. R., Tang, Q., Wolfe, J. D., Abeshu, G.,  
551 Anantharaj, V., Asay-Davis, X. S., Bader, D. C., Baldwin, S. A., Bisht, G., Bogenschutz, P. A.,  
552 Branstetter, M., Brunke, M. A., Brus, S. R., Burrows, S. M., Cameron-Smith, P. J., Donahue, A.  
553 S., ... Zhu, Q. (2019). The DOE E3SM Coupled Model Version 1: Overview and Evaluation at  
554 Standard Resolution. *Journal of Advances in Modeling Earth Systems*, 11(7), 2089–2129.  
555 <https://doi.org/10.1029/2018MS001603>
- 556 Golaz, J.-C., Van Roekel, L. P., Zheng, X., Roberts, A. F., Wolfe, J. D., Lin, W., Bradley, A. M., Tang,  
557 Q., Maltrud, M. E., Forsyth, R. M., Zhang, C., Zhou, T., Zhang, K., Zender, C. S., Wu, M.,  
558 Wang, H., Turner, A. K., Singh, B., Richter, J. H., ... Bader, D. C. (2022). The DOE E3SM  
559 Model Version 2: Overview of the Physical Model and Initial Model Evaluation. *Journal of*



- 560 *Advances in Modeling Earth Systems*, 14(12), e2022MS003156.  
561 <https://doi.org/10.1029/2022MS003156>
- 562 Han, Y., Zhang, G. J., Huang, X., & Wang, Y. (2020). A Moist Physics Parameterization Based on Deep  
563 Learning. *Journal of Advances in Modeling Earth Systems*, 12(9), e2020MS002076.  
564 <https://doi.org/10.1029/2020MS002076>
- 565 Hartmann, D. L., Blossey, P. N., & Dygert, B. D. (2019). Convection and Climate: What Have We  
566 Learned from Simple Models and Simplified Settings? *Current Climate Change Reports*, 5(3),  
567 196–206. <https://doi.org/10.1007/s40641-019-00136-9>
- 568 Hourdin, F., Mauritsen, T., Gettelman, A., Golaz, J.-C., Balaji, V., Duan, Q., Folini, D., Ji, D., Klocke,  
569 D., Qian, Y., Rauser, F., Rio, C., Tomassini, L., Watanabe, M., & Williamson, D. (2017). The Art  
570 and Science of Climate Model Tuning. *Bulletin of the American Meteorological Society*, 98(3),  
571 589–602. <https://doi.org/10.1175/BAMS-D-15-00135.1>
- 572 Huang, H., Xue, Y., Li, F., & Liu, Y. (2020). Modeling long-term fire impact on ecosystem  
573 characteristics and surface energy using a process-based vegetation–fire model SSiB4/TRIFFID-  
574 Fire v1.0. *Geoscientific Model Development*, 13(12), 6029–6050. [https://doi.org/10.5194/gmd-13-](https://doi.org/10.5194/gmd-13-6029-2020)  
575 [6029-2020](https://doi.org/10.5194/gmd-13-6029-2020)
- 576 Huang, H., Xue, Y., Liu, Y., Li, F., & Okin, G. S. (2021). Modeling the short-term fire effects on  
577 vegetation dynamics and surface energy in southern Africa using the improved SSiB4/TRIFFID-  
578 Fire model. *Geoscientific Model Development*, 14(12), 7639–7657. [https://doi.org/10.5194/gmd-](https://doi.org/10.5194/gmd-14-7639-2021)  
579 [14-7639-2021](https://doi.org/10.5194/gmd-14-7639-2021)
- 580 Kochkov, D., Yuval, J., Langmore, I., Norgaard, P., Smith, J., Mooers, G., Lottes, J., Rasp, S., Düben, P.,  
581 Klöwer, M., Hatfield, S., Battaglia, P., Sanchez-Gonzalez, A., Willson, M., Brenner, M. P., &  
582 Hoyer, S. (2023). *Neural General Circulation Models* (arXiv:2311.07222). arXiv.  
583 <http://arxiv.org/abs/2311.07222>



- 584 Kondylatos, S., Prapas, I., Ronco, M., Papoutsis, I., Camps-Valls, G., Piles, M., Fernández-Torres, M.-Á.,  
585 & Carvalhais, N. (2022). Wildfire Danger Prediction and Understanding With Deep Learning.  
586 *Geophysical Research Letters*, 49(17), e2022GL099368. <https://doi.org/10.1029/2022GL099368>
- 587 Krasnopolsky, V. M., Fox-Rabinovitz, M. S., & Belochitski, A. A. (2013). Using ensemble of neural  
588 networks to learn stochastic convection parameterizations for climate and numerical weather  
589 prediction models from data simulated by a cloud resolving model. *Advances in Artificial Neural*  
590 *Systems*, 2013, 5–5. <https://doi.org/10.1155/2013/485913>
- 591 Lee, M.-I., Schubert, S. D., Suarez, M. J., Held, I. M., Lau, N.-C., Ploshay, J. J., Kumar, A., Kim, H.-K.,  
592 & Schemm, J.-K. E. (2007). An Analysis of the Warm-Season Diurnal Cycle over the Continental  
593 United States and Northern Mexico in General Circulation Models. *Journal of*  
594 *Hydrometeorology*, 8(3), 344–366. <https://doi.org/10.1175/JHM581.1>
- 595 Li, F., Zhu, Q., Riley, W. J., Zhao, L., Xu, L., Yuan, K., Chen, M., Wu, H., Gui, Z., Gong, J., &  
596 Randerson, J. T. (2023). AttentionFire\_v1.0: Interpretable machine learning fire model for  
597 burned-area predictions over tropics. *Geoscientific Model Development*, 16(3), 869–884.  
598 <https://doi.org/10.5194/gmd-16-869-2023>
- 599 O’Gorman, P. A., & Dwyer, J. G. (2018). Using machine learning to parameterize moist convection:  
600 Potential for modeling of climate, climate change, and extreme events. *Journal of Advances in*  
601 *Modeling Earth Systems*, 10(10), 2548–2563. <https://doi.org/10.1029/2018ms001351>
- 602 Randall, D. A. (2013). Beyond deadlock. *Geophysical Research Letters*, 40(22), 5970–5976.  
603 <https://doi.org/10.1002/2013GL057998>
- 604 Randall, D., Khairoutdinov, M., Arakawa, A., & Grabowski, W. (2003). Breaking the Cloud  
605 Parameterization Deadlock. *Bulletin of the American Meteorological Society*, 84(11), 1547–1564.  
606 <https://doi.org/10.1175/BAMS-84-11-1547>
- 607 Rasp, S., Pritchard, M. S., & Gentine, P. (2018). Deep learning to represent subgrid processes in climate  
608 models. *Proceedings of the National Academy of Sciences*, 115(39), 9684–9689.  
609 <https://doi.org/10.1073/pnas.1810286115>





- 610 Schär, C., Fuhrer, O., Arteaga, A., Ban, N., Charpiloz, C., Girolamo, S. D., Hentgen, L., Hoefler, T.,  
611 Lapillonne, X., Leutwyler, D., Osterried, K., Panosetti, D., Rüdüsühli, S., Schlemmer, L.,  
612 Schulthess, T. C., Sprenger, M., Ubbiali, S., & Wernli, H. (2020). Kilometer-Scale Climate  
613 Models: Prospects and Challenges. *Bulletin of the American Meteorological Society*, *101*(5),  
614 E567–E587. <https://doi.org/10.1175/BAMS-D-18-0167.1>
- 615 Swann, H. (2001). Evaluation of the mass-flux approach to parametrizing deep convection. *Quarterly*  
616 *Journal of the Royal Meteorological Society*, *127*(574), 1239–1260.  
617 <https://doi.org/10.1002/qj.49712757406>
- 618 Walters, D., Boutle, I., Brooks, M., Melvin, T., Stratton, R., Vosper, S., Wells, H., Williams, K., Wood,  
619 N., Allen, T., Bushell, A., Copsey, D., Earnshaw, P., Edwards, J., Gross, M., Hardiman, S.,  
620 Harris, C., Heming, J., Klingaman, N., ... Xavier, P. (2017). The Met Office Unified Model  
621 Global Atmosphere 6.0/6.1 and JULES Global Land 6.0/6.1 configurations. *Geoscientific Model*  
622 *Development*, *10*(4), 1487–1520. <https://doi.org/10.5194/gmd-10-1487-2017>
- 623 Wang, S. S.-C., Leung, L. R., & Qian, Y. (2023). Projection of Future Fire Emissions Over the  
624 Contiguous US Using Explainable Artificial Intelligence and CMIP6 Models. *Journal of*  
625 *Geophysical Research: Atmospheres*, *128*(14), e2023JD039154.  
626 <https://doi.org/10.1029/2023JD039154>
- 627 Wang, S. S.-C., Qian, Y., Leung, L. R., & Zhang, Y. (2022). Interpreting machine learning prediction of  
628 fire emissions and comparison with FireMIP process-based models. *Atmospheric Chemistry and*  
629 *Physics*, *22*(5), 3445–3468. <https://doi.org/10.5194/acp-22-3445-2022>
- 630 Wang, X., Han, Y., Xue, W., Yang, G., & Zhang, G. J. (2022). Stable climate simulations using a realistic  
631 general circulation model with neural network parameterizations for atmospheric moist physics  
632 and radiation processes. *Geoscientific Model Development*, *15*(9), 3923–3940.  
633 <https://doi.org/10.5194/gmd-15-3923-2022>



- 634 Webster, S., Uddstrom, M., Oliver, H., & Vosper, S. (2008). A high-resolution modelling case study of a  
635 severe weather event over New Zealand. *Atmospheric Science Letters*, 9(3), 119–128.  
636 <https://doi.org/10.1002/asl.172>
- 637 Xu, K.-M., & Randall, D. A. (1996). A Semiempirical Cloudiness Parameterization for Use in Climate  
638 Models. *Journal of the Atmospheric Sciences*, 53(21), 3084–3102. [https://doi.org/10.1175/1520-0469\(1996\)053<3084:ASCPFU>2.0.CO;2](https://doi.org/10.1175/1520-0469(1996)053<3084:ASCPFU>2.0.CO;2)
- 640 Zhang, T., Lin, W., Vogelmann, A. M., Zhang, M., Xie, S., Qin, Y., & Golaz, J.-C. (2021). Improving  
641 Convection Trigger Functions in Deep Convective Parameterization Schemes Using Machine  
642 Learning. *Journal of Advances in Modeling Earth Systems*, 13(5), e2020MS002365.  
643 <https://doi.org/10.1029/2020MS002365>
- 644 Zhang, T., Morcrette, C., Zhang, M., Lin, W., Xie, S., Liu, Y., Weverberg, K. V., & Rodrigues, J. (2024).  
645 *tzhang-ccs/ML4ESM: ML4ESM\_v1* (Version v1) [Computer software].  
646 <https://doi.org/10.5281/ZENODO.11005103>
- 647